Saengsin *et al. Journal of Orthopaedic Surgery and Research* (2025) 20:254
https://doi.org/10.1186/s13018-025-05645-y

Journal of Orthopaedic Surgery and Research

RESEARCH **Open Access**

Ultrasonography for diagnosing medial sided ankle instability in supination external rotation ankle fracture

Jirawat Saengsin[1,2*], Pongpanot Sornsakrin[1], Pichitchai Atthakomol[2], Go Sato[1,3], Bart Lubberts[1,4], Gregory Waryasz[1,4], Christopher W. DiGiovanni[4,5] and Daniel Guss[4,5]

Abstract

Background Destabilizing injuries to the deltoid ligament have relied on radiographic stress examination for diagnosis, with a focus on medial clear space widening. Increasingly, Portable ultrasound has also been used in the clinical setting, allowing dynamic and non-invasive evaluation at the point of care. The aim of this study was to determine whether portable ultrasound can detect medial sided instability associated with supination-external rotation type ankle injuries during the gravity stress, weightbearing, and external rotation stress.

Methods Ten fresh-frozen cadaveric ankles were used in this study. Assessment of medial clear space distances with portable ultrasound was first performed with all structures intact, and later with sequential transection of the anterior inferior tibiofibular ligament (Stage I), Weber B fibular fracture (Stage II), posterior inferior tibiofibular ligament (Stage III), superficial deltoid ligament (Stage IVa), and the deep deltoid ligament (Stage IVb). In all scenarios, four loading conditions were considered; (1) a gravity stress test with the ankle positioned in a neutral position; (2) a gravity stress test with the ankle positioned in a plantarflexed position; (3) an external rotation stress test; and (4) simulated weightbearing condition.

Results Among all four loading conditions, all medial clear space values increased as the supination-external rotation ankle injury stage progressed (Spearman's rank correlation ranged from 0.43 to 0.90, $P<.001$). The medial clear space values measured with the portable ultrasound during; (1) gravity stress test in neutral ankle position, (2) gravity stress test in plantarflexed ankle position, (3) weightbearing, and (4) external rotation stress test were significantly increased between intact stage vs. stage IVb ($P=.036$), as well as between stage III vs. IVb (P ranged from 0.015 to 0.047).

Conclusions Portable ultrasonography is a feasible tool for diagnosing medial ankle instability in supination-external rotation ankle injury. The medial clear space measurements assessed with portable ultrasound during the gravity stress test, weightbearing, and the external rotation stress test well correlated with the supination-external rotation ankle injury staging. Besides, the portable ultrasound method can differentiate the supination-external rotation ankle injury stage IVb from the intact stage, as well as differentiating the supination-external rotation ankle fracture without deltoid ligament injury (III) from the supination-external rotation stage with complete deltoid ligament injury (IVb).

*Correspondence:
Jirawat Saengsin
Jsaengsin@gmail.com
Full list of author information is available at the end of the article

Keywords Ankle fracture, Deltoid ligament, Ultrasound, Medial clear space, Ankle instability

Introduction

The critical treatment distinction in supination external rotation (SER) ankle fractures lies in the ability to identify whether the injury has rendered the ankle unstable. In the setting of a displaced bimalleolar fracture, or when the tibiotalar joint is clearly subluxated, operative treatment is strongly recommended [1–4]. In the setting of an isolated lateral malleolar fracture, however, stability is predicated by whether the deep deltoid ligament is intact [5]. The deep deltoid ligament is critical towards preventing lateral talar shift and external rotation of the talus. Still, numerous studies have demonstrated that patient symptoms, physical examination, and static imaging techniques are not able to accurately diagnose the injury of the deltoid that results in medial ankle instability [5–9].

Several imaging modalities that do allow for a dynamic examination are currently being used to diagnose medial sided ankle instability. Manual external rotation stress radiographs, gravity stress radiographs, and weightbearing radiographs are commonly used techniques [5, 7, 10–14]. However, there is no consensus on which loading condition is considered the best for evaluating medial ankle instability in SER ankle injuries and current clinical practice varies based on clinician preference [1, 15–17]. With advances in ultrasound technology, including improved accuracy of image details as well as the ability to provide dynamic, multiplanar, real-time films, the potential for evaluating musculoskeletal conditions is rapidly increasing. Few studies have explored the feasibility and accuracy of the US examination of the deltoid ligament in the setting of ankle fractures showing promising results [18–20]. However, these studies explored the injured vs. uninjured state of the deltoid ligaments, such as fluid, hematoma, discontinuity of the ligament, and did not assess the ability of ultrasound to diagnose medial-sided ankle instability related to ligament injury.

Currently, no study has used ultrasound to dynamically evaluate the medial clear space (MCS) of the ankle when performing a gravity stress test (GST), an external rotation stress test or with weightbearing. As a predicate to using ultrasound to diagnose tibiotalar instability after an SER ankle fracture, we developed a novel ultrasound evaluation technique aiming to quantify medial ankle instability using ultrasound. This study aims to perform such measurements during the GST, external rotation stress test, and weightbearing in a cadaveric model of SER ankle injuries to (1) identify the relationship between the ultrasonographic MCS measurements and a sequentially created SER ankle injury model, (2) evaluate if the ultrasonography can detect a difference in MCS distance between an uninjured ankle and an SER injury type IV, and (3) investigate if the ultrasonographic MCS measurements can differentiate between the SER ankle injury with and without complete deltoid ligament rupture, as well as between the SER ankle injury with partial deltoid ligament injury and with complete deltoid ligament rupture. We hypothesize that there is a correlation between the ultrasonographic MCS measurements, and the sequentially created SER ankle injury model. We also hypothesize that there is an increase in ultrasonographic MCS distances between the uninjured ankle and the ankle with SER type IV injury, as well as between the SER ankle injury with and without complete deltoid ligament rupture, and between the SER ankle injury with partial deltoid ligament rupture and with complete deltoid ligament rupture when measured with the ultrasound.

Methods

Specimen preparation

Ten fresh-frozen below-knee amputated cadaveric specimens with intact proximal tibiofibular joint. The mean age at the time of death was 46 (range 32 to 56) years. Five were males, and five were females. Specimens were thawed at room temperature 24 h prior to the start of the experiment. Bone and soft tissue were carefully handled and maintained to simulate in vivo conditions. Before testing, ankle fluoroscopic images (anteroposterior, lateral, and mortise) were obtained in each specimen. In case a specimen showed signs of previous ankle trauma or severe degenerative changes, the cadaver was excluded from the study.

Sequential transection of ligaments or bones and loading conditions

All specimens underwent an identical sequence of ligamentous and bony transection. The assessment was performed first with all ankle ligaments and fibula intact and later with sequential transection of the anterior inferior tibiofibular ligament (AITFL) (SER injury stage I), Weber B fibular fracture (SER injury stage II), the posterior inferior tibiofibular ligament (PITFL) (SER injury stage III), the superficial deltoid ligament (SER injury stage IVa), and the deep deltoid ligament (SER injury stage IVb) [21, 22]. In all scenarios, four loading conditions were considered, including a GST in ankle neutral position, a GST in ankle plantarflexed position, an external rotation stress test, and weightbearing.

Description of the ultrasonographic gravity stress test

To perform the GST, the specimen was placed in a lateral decubitus position with the most distal half of the leg, ankle, and foot off the end of the table, allowing the weight of the foot and ankle to create a lateral force across the ankle joint [12, 23]. The measurements were obtained with the ankle held in neutral dorsiflexion (0 degrees) as well as with the ankle plantarflexed (15 degrees) [24]. An electronic goniometer was used to ensure that the ankle position was set and standardized in a proper position during the test (Fig. 1A and B).

Description of the ultrasonographic weightbearing

Simulated weightbearing with an axial load force of 750 N was performed. The amount of force used in this study was based on previous cadaveric studies [25, 26]. The 750 N axial loading force, which corresponds to 150 kg of weight for a two-legged stance, would represent the upper limit of weightbearing conditions for most individuals. The force was applied through a wooden block that was attached to the tibial plateau of the specimen (Fig. 1C). All applied forces were measured and standardized using a digital force gauge DFS2-R-0200 with an accuracy of 0.1% of full scale.

Description of the ultrasonographic external rotation stress test

Before testing, specimens were secured to a board beneath the leg with the use of two 5.0-mm Schanz pins placed from anterior to posterior into the proximal, middle third of the tibia. An external rotation stress test of the ankle was performed under 45Nm torque. The force was applied to the foot using a bone hook with the ankle positioned in neutral dorsiflexion. The bone hook was placed medially at the first metatarsal shaft (Fig. 1D). The 45 N (4.5Nm torque) used in this study was based on previous literature [11, 27, 28], that concluded that 45 N was sufficient to detect the medial-sided ankle instability during the radiographic external rotation stress test without exceeding the level of rotational force that can cause a fibular fracture or further ligamentous damage [29].

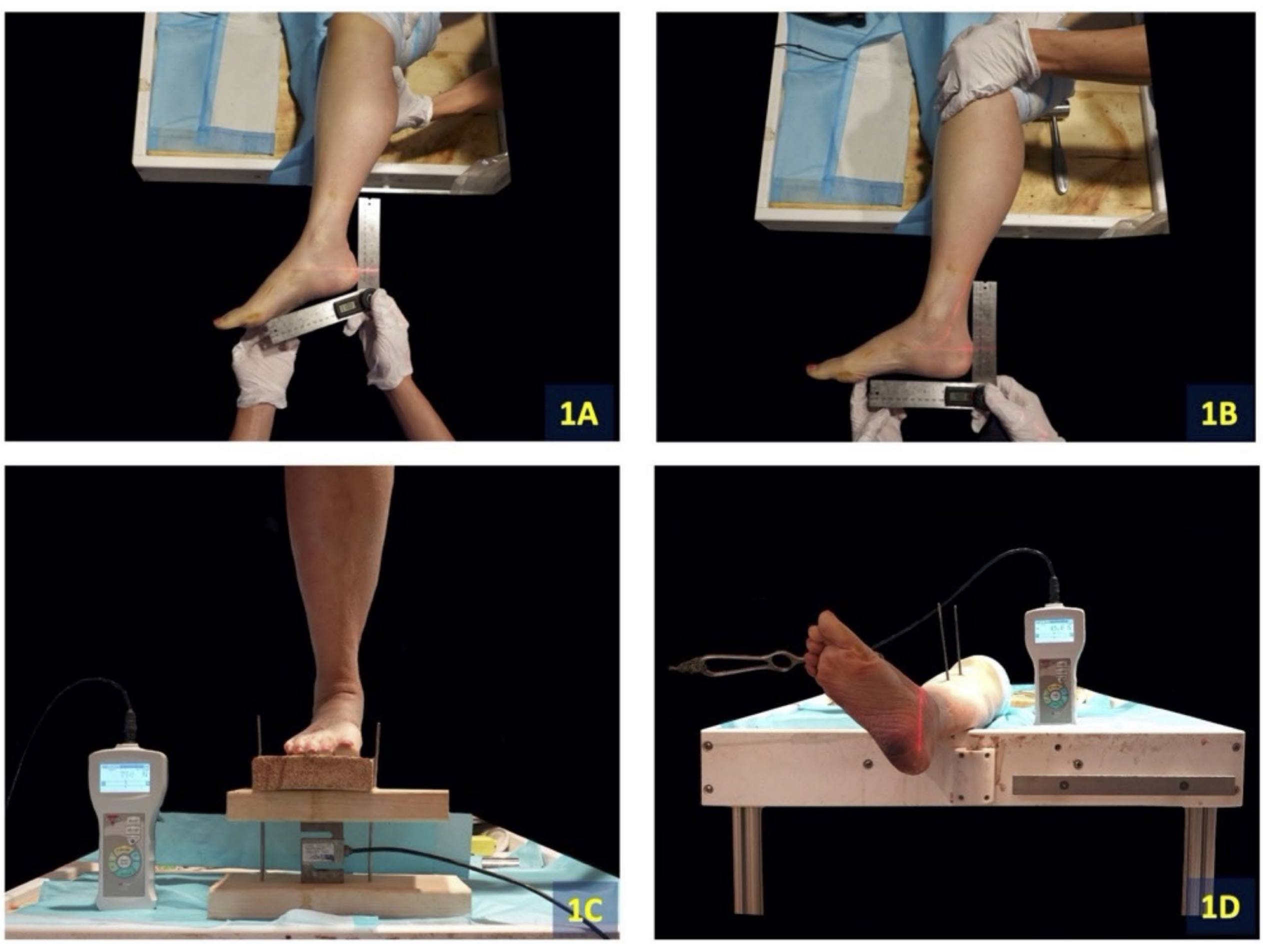

Fig. 1 Experimental setups during medial clear space evaluation
Loading experimental setups; 1 **A**) a gravity stress test in neutral ankle position, 1**B**) a gravity stress test in plantarflexed ankle position, 1 **C**) A simulated weightbearing with an axial load force of 750 N, 1**D**) An external rotation stress test under 45Nm torque

Ultrasonographic medial clear space measurement

In all loading scenarios, medial side assessment was performed using a portable ultrasound device (2D-gray scale B mode, Butterfly IQ ultrasound device, Butterfly Network, USA). The ultrasound images were taken using Butterfly IQ-Ultrasound software Version 1.15.0. Subsequently, Image J program (NIH, Bethesda, Maryland, USA).

was used to measure the MCS distances from the recorded P-US images. Three different MCS measurement values, including anterior-perpendicular-MCS, anterior-oblique-MCS, and inferior-MCS, were considered in this study accordingly to three planes of talar motion. During each stress maneuver, the anterior-perpendicular-MCS measured with the P-US represents the lateral shift of the talus. The anterior-oblique-MCS measured with the P-US represents the talar external rotation. The inferior-MCS measured with the P-US represents the talar eversion.

Prior to P-US examination, the landmarks for ultrasound probe positioning were identified. After mounting the cadaveric. Specimens, the fluoroscopy was used to find the tibiotalar joint line level (Fig. 2A). A marker was then used to draw two lines, one along the joint line level and another at about 1 cm below and parallel to the joint line level (Fig. 2B). To measure the MCS using P-US, the line representing 1 cm below joint line level was used as a first landmark for assessing the MCS from the anteromedial aspect of the ankle joint with the middle of the P-US probe positioned on this line and perpendicular to the medial gutter. At this anteromedial landmark, the anterior-perpendicular-MCS and anterior-oblique-MCS were evaluated on a transverse plane using the P-US. Then, the fluoroscopy was used to define the second landmark as the furthest distance from the joint line level at which the medial malleolus still articulated with the talus. At this inferomedial landmark, the inferior-MCS distance was assessed on a coronal plane using the P-US with the middle of the probe positioned perpendicular to this defined point (Fig. 2C).

When evaluated from the anteromedial aspect of the ankle joint (Fig. 3A), the anterior-perpendicular-MCS distance was measured from the transverse P-US images as represented by the perpendicular distance, drawn starting from the lateral border of the medial malleolus's hyperechoic bone contours to the medial border of the talus's hyperechoic bone contours (Fig. 3B and C). This anterior-perpendicular-MCS distance represents the

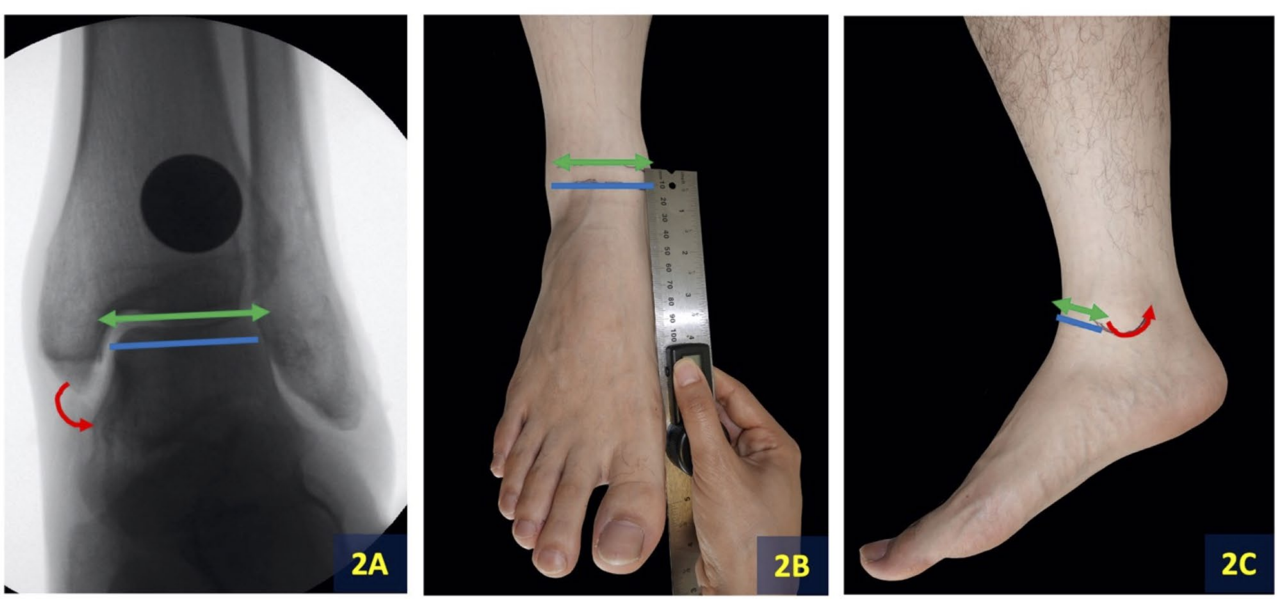

Fig. 2 Identification of ankle joint line level and landmark for the portable ultrasound assessment
2 **A**) The tibiotalar joint line is defined using fluoroscopy and labeled with a marker pen
2 **B**) Two lines are drawn, one along the joint line level (two-headed arrows) and another at about 1 cm below and parallel to the joint line level (thick line). The following line is used as a first landmark for assessing the MCS from the anteromedial aspect of the ankle joint with the middle of the P-US probe positioned on this line and perpendicular to the medial gutter
2 **C**) The tip of the medial malleolus is identified and outlined using fluoroscopy. The medial malleolar tip, where the furthest distance from the joint line level at which the medial malleolus still articulated with the talus, is used as a landmark for assessing the MCS from the inferomedial aspect of the ankle joint with the middle of the P-US probe placed perpendicular to this landmark
Two-headed arrows represent the ankle joint line level. Thick lines represent the landmark for the anteromedial aspect assessment. One-headed arrow represent the landmark for the inferomedial aspect assessment
(Abbreviations: MCS, medial clear space; P-US, portable ultrasound)

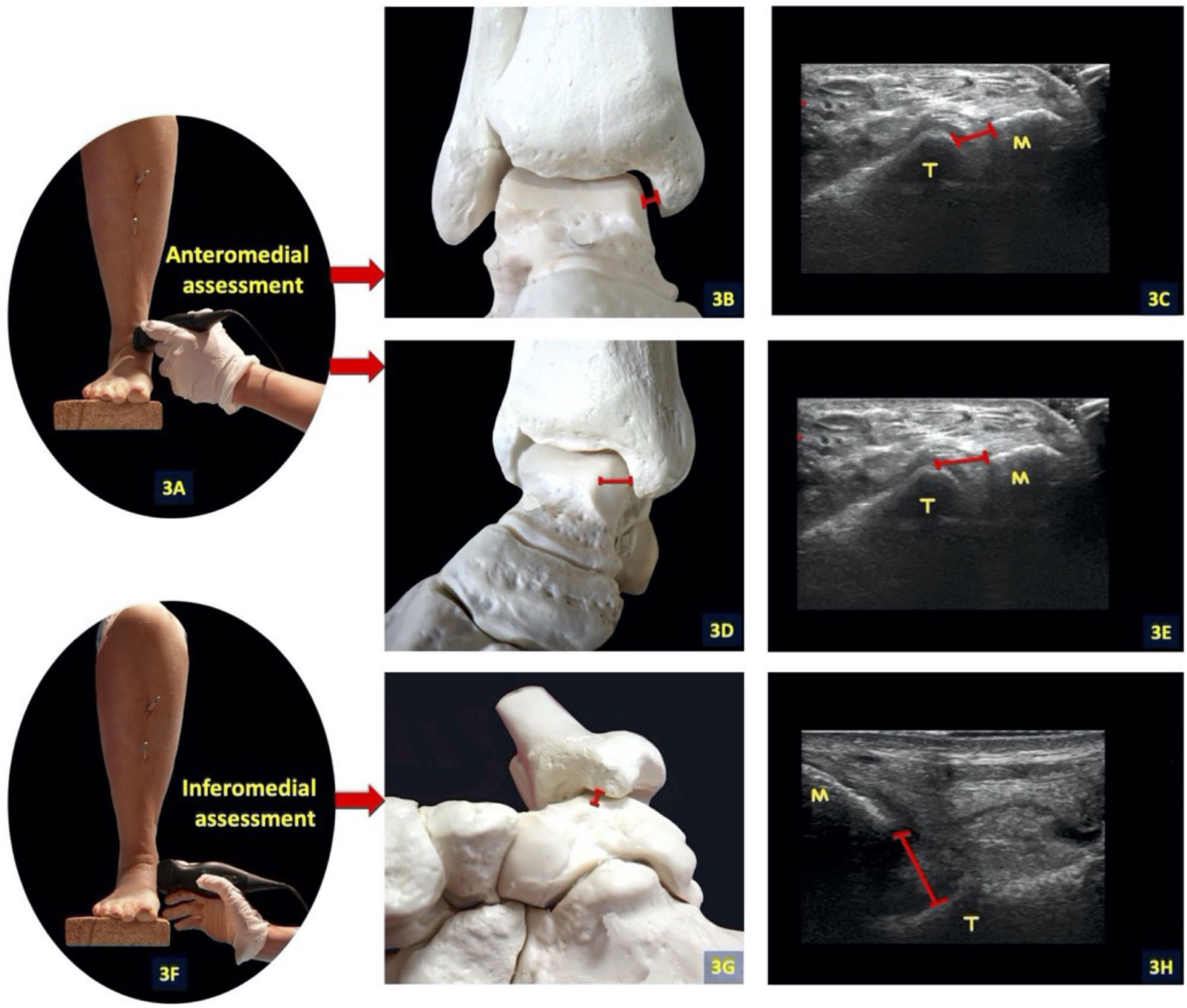

Fig. 3 P-US probe positioning and medial clear space distance measurements
3 **A**) The P-US probe was placed perpendicular to the anteromedial aspect of the medial gutter at the defined landmark for assessing the anterior-perpendicular-MCS and anterior-oblique-MCS. The anterior-perpendicular-MCS distance was measured in mm as represented by the perpendicular distance, drawn starting from the medial border of the talus's hyperechoic bone contour to the lateral border of the medial malleolus's hyperechoic bone contour (3 **B**, 3 **C**). The anterior-oblique-MCS distance was measured in mm as represented by the oblique distance drawn starting from the lateral border of the medial malleolus's hyperechoic bone contours to the anteromedial edge of the talus's hyperechoic bone contours (3 **D**, 3 **E**)
3 **F**) The P-US probe was placed perpendicular to the inferomedial aspect of the medial gutter at the defined landmark for assessing the inferior-MCS. The inferior-MCS distances were measured in mm as represented by the perpendicular distances, drawn starting from the medial border of the talus's hyperechoic bone contours at the level of the medial malleolar tip to the lateral border of the medial malleolus's hyperechoic bone contours Fig. 3**G**, 3**H**)
Thick lines represent MCS distances
(Abbreviations: MCS, medial clear space; M, medial malleolus; T, Talus; P-US, portable ultrasound)

lateral talar translation. With the same ultrasonographic image, the anterior-oblique-MCS distance was also measured in mm as represented by the oblique distance drawn starting from the lateral border of the medial malleolus's hyperechoic bone contours to the anteromedial edge of the talus's hyperechoic bone contours (Fig. 3D and E). This anterior-oblique-MCS distance represents the talar external rotation.

When evaluated from the inferomedial aspect of the ankle joint (Fig. 3F), the inferior-MCS distances were measured from the coronal P-US images as represented by the perpendicular distances, drawn starting from the medial border of the talus's hyperechoic bone contours at the level of the medial malleolar tip to the lateral border of the medial malleolus's hyperechoic bone contours (Fig. 3G and H). This inferior-MCS distance represents the talar eversion.

Reproducibility and reliability assessment

To assess the interobserver reliability of the P-US measurements, two orthopedic foot and ankle surgeons independently performed the MCS measurements in three randomly selected specimens. After three months, the recorded ultrasonographic MCS images of the three specimens were remeasured by the same orthopedic surgeons to assess the intraobserver reliability. From this data, the inter and intraobserver reliability was assessed using the interclass correlation coefficients (ICC) derived from a two-way mixed effects model analysis of variance for absolute agreement. A two-way mixed effects model was used, because the two observers were not randomly selected, and both observers scanned the same subjects. Interpretation of the ICC values were interpreted as follows: ICC < 0.4, poor; 0.4 < ICC < 0.59, acceptable; 0.6 < ICC < 0.74, good; and ICC > 0.74, excellent [30].

Statistical analysis

All MCS measurements were reported with median and interquartile range (IQR) in millimeter (mm). The data of the intact joint in each loading condition was designated as the baseline value. To investigate the correlation between the ultrasonographic MCS measurements and the SER ankle injury stages, a Spearman's rank correlation was used. In order to achieve 90% statistical power for detecting a correlation with large effect size (r = .5) between the ultrasonographic MCS measurements and the SER ankle injury stages with an overall two-tailed type-1 rate of 2.5%, we would need a minimum of 48 observations. In each specimen, the ultrasonographic MCS measurements were measured in the intact state, as well as in five SER ankle injury stages, resulting in six observations. Thus, to answer the hypothesis, we would need eight specimens. Accounting for 20% exclusion of specimen due to signs of previous ankle trauma or severe degenerative changes, the total amount included in this study was 10 specimens.

To detect a difference in measured MCS distances for each stress test and each injury stage to the intact stage, a Wilcoxon signed-rank test was performed for each imaging modality. P values were adjusted for multiple comparison using the Holm-Bonferroni method. A 2-sided P value of less than 0.05 was considered statistically significant. The sample size calculation was based on the previous cadaveric study by Ashraf et al. [21] investigated MCS values using radiographic images of the ankle in a neutral position in a gravity stress test condition and found a mean and standard deviation (SD) of 4.33 ± 0.72 mm for the SER ankle injury stage III-b (with only superficial deltoid rupture) and a mean and SD of 7.11 ± 1.03 mm for the SER ankle injury stage IV (with complete deltoid rupture). In order to achieve 95% statistical power for detecting a difference of 2.78 mm in MCS distances (4.33 ± 0.72 vs. 7.11 ± 1.03 mm, 0.3 correlation) among the MCS measurements, with an overall two-tailed Type-1 rate of 2.5% for a Wilcoxon signed-rank test, we need at least six specimens. The sample size calculation was performed using G*Power Version 3.1.9.4. All analyses were performed with Stata 13.0 for Mac (StataCorp LP, College Station, TX, USA).

Results

MCS values measured with the P-US increased as the SER ankle injury stage progressed. The Spearman's rank correlation coefficient ranged from 0.43 to 0.90 (P <.001), which indicate moderate to strong positive correlations between the ultrasonographic MCS measurements and the sequentially created supination-external rotation ankle injury model (Table 1).

All MCS values, including the anterior-perpendicular MCS, anterior-oblique MCS, and inferior MCS measured

Table 1 Correlation between portable ultrasound measurements and sequentially created supination-external rotation ankle injury model

P-US vs. sequentially created SER ankle injury model	Spearman Rank Correlation	*P* Value
Anterior-perpendicular-MCS during GST-N	0.81	**< 0.001**
Anterior-perpendicular-MCS during GST-PF	0.77	**< 0.001**
Anterior-perpendicular-MCS during weightbearing	0.60	**< 0.001**
Anterior-perpendicular-MCS during ER stress test	0.85	**< 0.001**
Anterior-oblique-MCS during GST-N	0.79	**< 0.001**
Anterior-oblique-MCS during GST-PF	0.76	**< 0.001**
Anterior-oblique-MCS during weightbearing	0.43	**< 0.001**
Anterior-oblique-MCS during ER stress test	0.90	**< 0.001**
Inferior-MCS during GST-N	0.76	**< 0.001**
Inferior-MCS during GST-PF	0.77	**< 0.001**
Inferior-MCS during weightbearing	0.60	**< 0.001**
Inferior-MCS during ER stress test	0.82	**< 0.001**

Significant adjusted *P* values are in bold for Spearman's rank correlation

Abbreviations: P-US = portable ultrasound, SER = supination external rotation, GST-N = gravity stress test in neutral ankle position, GST-PF = gravity stress test in ankle plantarflexed position, ER = external rotation, MCS = medial clear space with the P-US during; (1) the GST in neutral ankle position, (2) the GST in plantarflexed ankle position, (3) weightbearing, and (4) the external rotation stress test, significantly increased between intact stage vs. stage IVb (P=.036) (Table 2). When compared between SER ankle injury stage III vs. IVb and stage IVa vs. IVb, the P-US MCS values measured during the GST and external rotation stress test significantly increased when the injury progressed from stage III to IVb (P ranged from 0.015 to 0.031) or from IVa to IVb (P ranged from 0.015 to 0.028) (Table 3). Notably, MCS values measured with the P-US during weightbearing were significantly increased only between intact stage vs. stage IVb (P=.036) and between stage III vs. stage IVb (P ranged from 0.031 to 0.047), but not between stage III vs. IVb (P ranged from 0.083 to 0.28). Interobserver (0.97; 95% confidence interval: 0.96 to 0.98) and intraobserver reliability (0.95; 95% confidence interval: 0.94 to 0.96) for the P-US MCS measurements were all substantial.

Discussion

In recent years, dynamic P-US is increasingly being used to evaluate musculoskeletal injuries at the point of care. The objectives of this cadaveric study were to assess the relationship between the ultrasonographic MCS measurements and a sequentially created SER ankle injury model, as well as to determine whether the dynamic ultrasonography can detect medial side instability in SER type ankle fracture. We found moderate to strong positive correlations between the P-US MCS measurements and the sequentially created SER ankle injury model for the assessment of medial ankle instability. By assessing the MCS using P-US during the GST, weightbearing, or the external rotation stress test, SER ankle fracture with complete deltoid ligament rupture (IVb) can be differentiated from the uninjured ankle or other SER ankle injury stages (I to IVa).

Results in the current study and data presented in previous literature confirmed that the deltoid ligaments contribute to tibiotalar joint stability on the medial side in the SER ankle fracture [1–5, 31, 32]. Most of the previous researches used radiographic imaging for assessing medial ankle instability in isolated fibular fracture. Correspondingly, we found that the MCS values as measured with the P-US increased as the SER ankle injury stage progressed and that these values significantly correlated with the SER injury staging (P<.001) (Table 1). Our findings underscore that ultrasonography has reached a level of technological maturity capable of evaluating medial side ankle injuries as an alternative to radiography. Prior studies have explored the feasibility and accuracy of using ultrasound to examine the deltoid ligament in the setting of ankle fractures [18–20]. These studies only examined the quality of the deltoid ligament, i.e., injury, including fluid, hematoma, discontinuity of the ligament, and evidence of articular pouch on the medial side of the ankle that approaches the tibialis posterior tendon. Although deltoid injury could be diagnosed with these ultrasonographic signs, this examination does not answer the fundamental question of whether the deltoid ligament injury has rendered the ankle unstable.

With our P-US evaluating technique, three planes of talar motion can be evaluated. During the stress maneuvers, the anterior-perpendicular-MCS measured with the P-US represents the lateral shift of the talus. The anterior-oblique-MCS measured with the P-US represents the talar external rotation. The inferior-MCS measured with the P-US represents the talar eversion. Our results found that, as the staging of injury progress, multidirectional instability on the medial side of the ankle, including lateral talar shift, talar external rotation and talar tilting occur simultaneously (Table 1).

Notably, the correlations found between the MCS values measured during weightbearing vs. the injury staging were moderate (r ranged from 0.43 to 0.60), while the correlations were strong when the MCS values were measured during the GST and external rotation stress test (r ranged from 0.76 to 0.90). This is likely due to the difference in forces applied to the ankle during the stress maneuvers. According to the concept of Lauge-Hansen SER ankle fracture [31], the injury results from the rotational force that renders ligamentous and bony damage in a circular pattern starting from the lateral aspect, which is the AITFL to the medial aspect which is the deltoid ligament. As stress is applied to an injured ankle, the medial ankle instability, as represented by the MCS values, may gradually increase during the GST or external rotation stress test. These loading conditions likely simulate the ankle fractures mechanisms, which could result in a better correlation coefficient. In contrast, during weightbearing, the stability of the tibiotalar joint is likely provided by the bony congruency. The majority of force passes directly from the talar dome to the tibial plafond regardless of the presence of the fibular lateral buttress [17]. Stewart et al. performed a cadaveric study to evaluate the effect of deltoid incompetence on the stability of ankle mortise with an applied axial loading [16]. They found that the weightbearing radiographs cannot illustrate medial-sided ankle instability as relative to the forces applied with the GST or manual external rotation stress test. Although the correlation between the MCS values measured during weightbearing vs. the sequentially created SER ankle injury model was moderate, as the injury progressed to the last stage (IVb), the MCS values increased and became significantly larger when compared to the uninjured stage (P=.036).

One critical consideration for the effective clinical care of patients with isolated lateral malleolar fractures is

Table 2 Portable ultrasonographic medial clear space measurements during the gravity stress test, weightbearing and the external rotation stress test in the sequentially created SER ankle injury model

SER injury Stage	Loading conditions	Anterior-perpendicular-MCS in mm (Median, IQR)	Adjusted *P* Value (vs. intact stage)	Inferior-MCS in mm (Median, IQR)	Adjusted *P* Value (vs. intact stage)	Anterior-oblique-MCS in mm (Median, IQR)	Adjusted *P* Value (vs. intact stage)
Intact	GST-N	3.5 (2.8–4.4)	Ref	3.7 (3.4–3.8)	Ref	6.9 (5.9–7.2)	Ref
	GST-PF	4.0 (3.7–4.4)	Ref	4.2 (3.9–4.7)	Ref	8.6 (8.1–9.1)	Ref
	Weightbearing	3.0 (1.9–3.4)	Ref	2.7 (2.2–3.2)	Ref	4.9 (4.5–5.8)	Ref
	ER stress test	3.7 (3.2–4.6)	Ref	4.3 (3.9–4.5)	Ref	7.1 (6.1–7.5)	Ref
I	GST-N	4.0 (3.4–4.5)	0.11	3.8 (3.7–4.7)	0.33	7.4 (6.2–8.5)	0.24
	GST-PF	4.5 (3.5–5.3)	0.24	4.6 (3.5–5.2)	0.24	8.1 (6.8–9.4)	0.96
	Weightbearing	3.1 (2.8–3.4)	0.20	2.9 (2.6–4.3)	0.20	5.2 (4.1-6.0)	0.88
	ER stress test	4.6 (4.4–5.1)	**0.021**	6.3 (4.5–6.9)	**0.033**	7.9 (7.0-9.6)	**0.028**
II	GST-N	5.4 (4.6–6.7)	**0.044**	5.8 (5.0-6.4)	**0.028**	8.7 (7.0-9.7)	0.094
	GST-PF	5.7 (5.5-6.0)	**0.014**	5.8 (4.7–7.3)	**0.044**	9.9 (9.5–11.1)	0.057
	Weightbearing	3.1 (2.4–3.9)	0.34	3.1 (2.7–3.5)	0.23	5.7 (5.5–6.1)	0.42
	ER stress test	7.5 (7.3–8.8)	**0.020**	7.1 (5.5–8.5)	**0.020**	14.1 (12.2–14.7)	**0.020**
III	GST-N	6.5 (5.7–6.7)	**0.026**	6.5 (5.9–7.6)	**0.028**	9.8 (9.5–10.8)	**0.026**
	GST-PF	6.4 (5.1–7.7)	**0.026**	6.6 (5.5–7.7)	**0.050**	10.7 (9.7–11.9)	**0.021**
	Weightbearing	3.4 (2.9-4.0)	0.11	3.5 (2.3–4.2)	0.37	5.5 (5.3–6.2)	0.19
	ER stress test	8.4 (7.5–10.0)	**0.026**	8.4 (7.6–9.8)	**0.026**	15.7 (13.3–16.2)	**0.026**
IVa	GST-N	7.4 (6.6–8.3)	**0.031**	6.5 (5.7–6.3)	**0.035**	11.3 (10.9–12.5)	**0.031**
	GST-PF	6.6 (6.4–7.4)	**0.031**	6.9 (6.0-8.7)	**0.037**	11.4 (10.0-12.4)	**0.028**
	Weightbearing	3.6 (3.1–4.5)	0.18	4.3 (3.2–5.5)	0.056	5.6 (4.3–6.8)	0.89
	ER stress test	10.3 (8.3–11.0)	**0.031**	10.2 (8.3–10.5)	**0.031**	15.8 (14.9–18.2)	**0.031**
IVb	GST-N	12.3 (10.5–14.4)	**0.036**	13.5 (11.5–16.0)	**0.036**	15.6 (14.3–18.3)	**0.036**
	GST-PF	13.1 (12.1–14.6)	**0.036**	12.4 (11.3–12.6)	**0.036**	19.0 (16.5–21.6)	**0.036**
	Weightbearing	4.9 (4.5–5.7)	**0.036**	5.2 (4.4–5.5)	**0.036**	7.4 (5.6–8.4)	**0.036**
	ER stress test	12.4 (10.0-16.5)	**0.036**	12.8 (10.8–15.6)	**0.036**	20.1 (19.3–22.5)	**0.036**

Significant adjusted *P* values are in bold for Wilcoxon signed-rank test with Holm-Bonferroni correction. Stage I = AITFL transection; Stage II = AITFL transection + Weber B fibular fracture; Stage III = AITFL transection + Weber B fibular fracture + PITFL transection; Stage IVa = AITFL transection + Weber B fibular fracture + PITFL transection + superficial deltoid transection; Stage IVb = AITFL transection + Weber B fibular fracture + PITFL transection + superficial deltoid transection + deep deltoid transection

Abbreviations: P-US = portable ultrasound; SER = supination external rotation; GST-N = gravity stress test in neutral ankle position; GST-PF = gravity stress test in ankle plantarflexed position; ER = external rotation, mm = millimeter; IQR = interquartile range; MCS = medial clear space; AITFL = anteroinferior tibiofibular ligament; PITFL = posteroinferior tibiofibular ligament; Ref = reference

Table 3 Portable ultrasonographic medial clear space measurements during the gravity stress test, weightbearing, and the external rotation stress test comparing between stage III vs. IVb and between stage IVa vs. IVb in the sequentially created SER ankle injury model

Loading conditions	SER injury Stage	Anterior-perpendicular-MCS in mm (Median, IQR)	Adjusted *P* Value (IVa vs. IVb)	Inferior-MCS in mm (Median, IQR)	Adjusted *P* Value (IVa vs. IVb)	Anterior-oblique-MCS in mm (Median, IQR)	Adjusted *P* Value (IVa vs. IVb)
GST-N	III	6.5 (5.7–6.7)	**0.020**	6.5 (5.9–7.6)	**0.031**	9.8 (9.5–10.8)	**0.028**
	IVa	7.4 (6.6–8.3)	**0.015**	6.5 (5.7–6.3)	**0.019**	11.3 (10.9–12.5)	**0.020**
	IVb	12.3 (10.5–14.4)	Ref	13.5 (11.5–16.0)	Ref	15.6 (14.3–18.3)	Ref
GST-PF	III	6.4 (5.1–7.7)	**0.020**	6.6 (5.5–7.7)	**0.031**	10.7 (9.7–11.9)	**0.031**
	IVa	6.6 (6.4–7.4)	**0.015**	6.9 (6.0-8.7)	**0.026**	11.4 (10.0-12.4)	**0.026**
	IVb	13.1 (12.1–14.6)	Ref	12.4 (11.3–12.6)	Ref	19.0 (16.5–21.6)	Ref
Weight bearing	III	3.4 (2.9-4.0)	**0.031**	3.5 (2.3–4.2)	**0.047**	5.5 (5.3–6.2)	**0.031**
	IVa	3.6 (3.1–4.5)	0.083	4.3 (3.2–5.5)	0.28	5.6 (4.3–6.8)	0.14
	IVb	4.9 (4.5–5.7)	Ref	5.2 (4.4–5.5)	Ref	7.4 (5.6–8.4)	Ref
ER stress test	III	8.4 (7.5–10.0)	**0.025**	8.4 (7.6–9.8)	**0.021**	15.7 (13.3–16.2)	**0.015**
	IVa	10.3 (8.3–11.0)	**0.028**	10.2 (8.3–10.5)	**0.022**	15.8 (14.9–18.2)	**0.010**
	IVb	12.4 (10.0-16.5)	Ref	12.8 (10.8–15.6)	Ref	20.1 (19.3–22.5)	Ref

Significant adjusted *P* values are in bold for Wilcoxon signed-rank test with Holm-Bonferroni correction. Stage IVa = AITFL transection + Weber B fibular fracture + PITFL transection + superficial deltoid transection; Stage IVb = AITFL transection + Weber B fibular fracture + PITFL transection + superficial deltoid transection + deep deltoid transection

Abbreviations: P-US = portable ultrasound, SER = supination external rotation, GST-N = gravity stress test in neutral ankle position, GST-PF = gravity stress test in ankle plantarflexed position, ER = extrenal rotation, mm = millimeter, IQR = interquartile range, MCS = medial clear space, AITFL = anteroinferior tibiofibular ligament, PITFL = posteroinferior tibiofibular ligament; Ref = reference

assessing whether a concomitant deltoid ligament injury has rendered the tibiotalar joint unstable. Our study paves the way for using the P-US to diagnose destabilizing deltoid injuries via the ultrasonographic MCS measurements. The current study found that all MCS values as measured with the P-US during the GST in ankle neutral or plantarflexed position, during weightbearing, and during the external rotation stress test were significantly different between the uninjured stage vs. SER injury stage IVb (P =.036), and between SER injury stage III vs. IVb (P ranged from 0.015 to 0.047).

These findings highlight the capability of the dynamic ultrasonography for diagnosing SER ankle fracture with complete deltoid ligament rupture, as well as the ability to differentiate the unstable [SER] injury from the intact state and the stable injuries. Previously, studies have demonstrated that physical examination, such as medial ecchymosis, swelling or tenderness, and static radiography are not accurate for diagnosing incompetence of the deltoid ligament in SER ankle fracture [5–9]. Therefore, the stress radiography during the GST, weightbearing, or the manual external rotation stress test is usually recommended [5, 7, 10–13]. However, stress radiography may not readily be available in out-patients clinics or resource-limited settings, and the test itself leads to a significant amount of radiation exposure to both patients and examiners. In contrast, the P-US, which is radiation-free and readily available in portable mode [19, 33–37], can be used to evaluate medial ankle instability at the point of care, as well as to assess the outcome after treatment and progression of the instability during the follow-up visit.

Interestingly, the MCS values measured with the P-US during the GST and the external rotation stress test significantly increased from the intact stage as the SER injury progressed to stage I or II (P ranged from 0.014 to 0.044). Based on these findings, the ultrasonographic GST and external rotation stress test may be too sensitive for estimating the medial ankle instability. Previous literature also supported this finding. A study by Koval et al. [38] reported a cohort of 21 patients with SER stage IV ankle fracture who were evaluated with an external rotation stress radiograph. They found that 90% of patients had only partial deltoid ligament tear when confirmed with magnetic resonance imaging. Recently, many studies found that the GST or external rotation stress radiographs may overdiagnose the unstable SER ankle fracture patients which could lead to an unnecessary surgery [39–42]. These studies compared the results of operative vs. nonoperative treatment in unstable SER ankle fractures that were diagnosed with the GST or external rotation stress radiographs. They found equivalent functional outcomes of operative and nonoperative management as assessed using patient-based outcome measurements, which raises a question on whether a positive GST or external rotation stress test is really an indication for surgery, or could it be that these stress maneuvers may overestimate the unstable injury.

In contrast, during weightbearing, the MCS values as measured with the P-US became significantly larger when compared to the uninjured stage only after the complete deltoid ligament ruptured (IVb) (P=.036), while there is no significantly increased in MCS values when the injury progress to stage III or stage IVa (P ranged from 0.056 to 0.89). The weightbearing stress ultrasonography may better predict the medial ankle instability and could be more specific to the SER ankle fracture with medial ankle instability. Several studies have demonstrated the utility of weightbearing radiographs for assessing mortise stability in SER ankle injury [13, 14, 42, 43]. If mortise alignment and stability are achieved during weightbearing radiographs, even with positive GST or external rotation stress test, patients will still do well with nonoperative treatment. A recent article review by Kwon et al. [44] also underscored the concept of mortise stability during the weightbearing radiograph, which can be used as a guide for a successful nonoperative treatment and avoid unnecessary surgery in patients with SER ankle fracture. Our findings and the evidence from previous literature highlighted the capability and values of the weightbearing stress for assessing medial ankle instability in SER ankle fracture. The interobserver and intraobserver reliability for all ultrasonographic MCS measurements were all excellent, which represents that the ultrasound assessment is reliable and reproducible for the medial ankle instability evaluation.

Our study has several limitations. First, being a cadaveric study, the soft tissue conditions differ from those seen in-vivo. However, to simulate in vivo conditions as best possible, specimen bone and soft tissue were carefully maintained. Second, our measurement technique involved an operator learning curve inherent to any new technology. Even though we aimed to develop a reliable assessment technique, an experienced operator is still needed for accurate image acquisition as changes or tilting in probe position may potentially cause measurement variability of MCS cortical margins secondary to off-axis transverse imaging of the MCS resulting in falsely elevated oblique transverse measurements. However, in the hands of an experienced operator, sonographic images can provide useful information without radiation or any other contraindication. Our experience is that an orthopaedic surgeon's knowledge of anatomy far supersedes any technical impediment to mastering this new technology. Third, we were unable to measure the tibiotalar plafond joint or the superior clear space as a relative comparison point for the MCS. This space is difficult to measure with the ultrasound since the shape of the superior clear space is a curved surface formed by the talar dome and distal end of the tibia. The sound wave from the ultrasound transducer is obscure by the distal tibia's anterior ridge, thus preventing us from getting the clear images at the dome of the talus. Finally, to adequately assess medial ankle instability using dynamic P-US, stress to the ankle is required, which might not be tolerated by the patient in the clinical setting. To address this, a care provider may prescribe pain medication or local analgesia prior to P-US evaluation.

Conclusion

The use of dynamic stress ultrasonography for diagnosing medial ankle instability in SER ankle injury appears to be a reliable and repeatable technique. The MCS measurements assessed with P-US during the GST, weightbearing, and the external rotation stress test significantly correlated with the SER ankle injury staging (P<.001). In addition, the P-US method is capable of differentiating the SER ankle injury stage IVb from the intact stage, as well as differentiating the stable SER ankle injury stage from the unstable stage. Therefore, the P-US can be a valuable diagnostic tool at the point of care due to its ability to dynamically evaluate suspected medial ankle instability in SER type injury.

Abbreviations

AITFL	Anterior inferior tibiofibular ligament
GST	Gravity stress test
ICC	Interclass correlation coefficients
IQR	Interquartile range
MCS	Medial clear space
mm	Millimeter
PITFL	Posterior inferior tibiofibular ligament
P-US	Portable ultrasound
SD	Standard deviation
SER	Supination external rotation

Acknowledgements

We gratefully acknowledge the Foot and Ankle Research and Innovation Lab, Massachusetts General Hospital, Harvard Medical School, Boston, MA for providing resource, the Butterfly Network. inc, and OrthoScan. inc for their nonfinancial research support during the conduct of the study.

Author contributions

J.S. designed the study, collected the data, analyzed the data and wrote the manuscript. P.S. designed the study, collected the data. P.A. interpreted the data and edited the manuscript. G.S. designed the study, collected the data and wrote the manuscript. B.L. designed the study, analyzed the data and wrote the manuscript. G.W. designed the study and wrote the manuscript. C.W.D. designed the study and wrote the manuscript. D.G. designed the study and wrote the manuscript. All authors have read and approved the final submitted manuscript.

Funding

The study was funded by the American Orthopaedic Foot and Ankle Society (AOFAS; Grant ID 2019-122-S).

Data availability

The datasets used and/or analysed during the current study are available from the corresponding author on reasonable request.

Declarations

Ethics approval and consent to participate

Ethical approval for this study was waived by Partners Human Research Committee because the IRB determined that this activity does not meet the definition of human subjects research and the investigators will not obtain data through an intervention or interaction with individual subjects or identifiable private information about living individuals.

Consent for publication

Not applicable.

Competing interests

The authors declare no competing interests.

Author details

[1]Foot and Ankle Research and Innovation Lab, Massachusetts General Hospital, Harvard Medical School, Boston, MA, USA
[2]Department of Orthopaedics, Faculty of Medicine, Chiang Mai University, Chiang Mai, Thailand
[3]Department of Orthopedic, Asahikawa medical university, Asahikawa, Hokkaido, Japan
[4]Foot & Ankle Service, Department of Orthopaedic Surgery, Massachusetts General Hospital Harvard Medical School, Boston, MA, USA
[5]Newton-Wellesley Hospital, Massachusetts General Hospital, Harvard Medical School, Boston, MA, USA

Received: 4 February 2025 / Accepted: 24 February 2025
Published online: 10 March 2025

References

1. Michelsen JD, Ahn UM, Helgemo SL. Motion of the ankle in a simulated supination-external rotation fracture model. J Bone Joint Surg Am. 1996;78(7):1024–31.
2. Clarke HJ, Michelson JD, Cox QG, Jinnah RH. Tibio-talar stability in bimalleolar ankle fractures: a dynamic in vitro contact area study. Foot Ankle. 1991;11(4):222–7.
3. Bauer M, Bergström B, Hemborg A, Sandegård J. Malleolar fractures: nonoperative versus operative treatment. A controlled study. Clin Orthop Relat Res. 1985;199:17–27.
4. Baird RA, Jackson ST. Fractures of the distal part of the fibula with associated disruption of the deltoid ligament. Treatment without repair of the deltoid ligament. J Bone Joint Surg Am. 1987;69(9):1346–52.
5. van den Bekerom MP, Mutsaerts EL, van Dijk CN. Evaluation of the integrity of the deltoid ligament in supination external rotation ankle fractures: a systematic review of the literature. Arch Orthop Trauma Surg. 2009;129(2):227–35.
6. DeAngelis NA, Eskander MS, French BG. Does medial tenderness predict deep deltoid ligament incompetence in supination-external rotation type ankle fractures? J Orthop Trauma. 2007;21(4):244–7.
7. Egol KA, Amirtharajah M, Amirtharage M, Tejwani NC, Capla EL, Koval KJ. Ankle stress test for predicting the need for surgical fixation of isolated fibular fractures. J Bone Joint Surg Am. 2004;86–A(11):2393–8.
8. Stufkens SA, van den Bekerom MP, Knupp M, Hintermann B, van Dijk CN. The diagnosis and treatment of deltoid ligament lesions in supination-external rotation ankle fractures: a review. Strategies Trauma Limb Reconstr. 2012;7(2):73–85.
9. Schuberth JM, Collman DR, Rush SM, Ford LA. Deltoid ligament integrity in lateral malleolar fractures: a comparative analysis of arthroscopic and radiographic assessments. J Foot Ankle Surg. 2004;43(1):20–9.
10. Gill JB, Risko T, Raducan V, Grimes JS, Schutt RC. Comparison of manual and gravity stress radiographs for the evaluation of supination-external rotation fibular fractures. J Bone Joint Surg Am. 2007;89(5):994–9.
11. McConnell T, Creevy W, Tornetta P. Stress examination of supination external rotation-type fibular fractures. J Bone Joint Surg Am. 2004;86–A(10):2171–8.
12. Michelson JD, Varner KE, Checcone M. Diagnosing deltoid injury in ankle fractures: the gravity stress view. Clin Orthop Relat Res. 2001(387):178–82.
13. Hoshino CM, Nomoto EK, Norheim EP, Harris TG. Correlation of weightbearing radiographs and stability of stress positive ankle fractures. Foot Ankle Int. 2012;33(2):92–8.
14. Weber M, Burmeister H, Flueckiger G, Krause FG. The use of weightbearing radiographs to assess the stability of supination-external rotation fractures of the ankle. Arch Orthop Trauma Surg. 2010;130(5):693–8.
15. Massri-Pugin J, Lubberts B, Vopat BG, Wolf JC, DiGiovanni CW, Guss D. Role of the deltoid ligament in syndesmotic instability. Foot Ankle Int. 2018;39(5):598–603.
16. Stewart C, Saleem O, Mukherjee DP, Suk M, Marymont J, Anissian L. Axial load weightbearing radiography in determining lateral malleolus fracture stability: a cadaveric study. Foot Ankle Int. 2012;33(7):548–52.
17. Lee S, Lin J, Hamid KS, Bohl DD. Deltoid ligament rupture in ankle fracture: diagnosis and management. J Am Acad Orthop Surg. 2019;27(14):e648–58.
18. Henari S, Banks LN, Radovanovic I, Radiovanovic I, Queally J, Morris S. Ultrasonography as a diagnostic tool in assessing deltoid ligament injury in supination external rotation fractures of the ankle. Orthopedics. 2011;34(10):e639–43.
19. Chen PY, Wang TG, Wang CL. Ultrasonographic examination of the deltoid ligament in bimalleolar equivalent fractures. Foot Ankle Int. 2008;29(9):883–6.
20. Rosa I, Rodeia J, Fernandes PX, Teixeira R, Saldanha T, Consciencia JG. Ultrasonographic assessment of deltoid ligament integrity in ankle fractures. Foot Ankle Int. 2020;41(2):147–53.
21. Ashraf A, Murphree J, Wait E, Winston T, Wooldridge A, Meriwether M, et al. Gravity stress radiographs and the effect of ankle position on deltoid ligament integrity and medial clear space measurements. J Orthop Trauma. 2017;31(5):270–4.
22. LAUGE-HANSEN N. Fractures of the ankle. II. Combined experimental-surgical and experimental-roentgenologic investigations. Arch Surg. 1950;60(5):957–85.
23. Jastifer JR, Jaykel M. Results of the gravity stress examination in the normal patient population. Foot Ankle Spec. 2017;10(5):398–401.
24. Saengsin J, Hagemeijer NC, Ho Chang S, Lubberts B, Waryasz G, Guss D et al. Medial ankle stability evaluation with dynamic ultrasound: Establishing natural variations in the healthy cohort. JAAOS - J Am Acad Orthop Surg. 9900;Publish Ahead of Print:https://doi.org/10.5435/JAAOS-D-20-00597
25. Goetz JE, Davidson NP, Rudert MJ, Szabo N, Karam MD, Phisitkul P. Biomechanical comparison of syndesmotic repair techniques during external rotation stress. Foot Ankle Int. 2018:1071100718786500.
26. Smith G, Mackenzie SP, Wallace RJ, Carter T, White TO. Biomechanical comparison of intramedullary fibular nail versus plate and screw fixation. Foot Ankle Int. 2017;38(12):1394–9.
27. Schock HJ, Pinzur M, Manion L, Stover M. The use of gravity or manual-stress radiographs in the assessment of supination-external rotation fractures of the ankle. J Bone Joint Surg Br. 2007;89(8):1055–9.
28. Park SS, Kubiak EN, Egol KA, Kummer F, Koval KJ. Stress radiographs after ankle fracture: the effect of ankle position and deltoid ligament status on medial clear space measurements. J Orthop Trauma. 2006;20(1):11–8.
29. Wei F, Villwock MR, Meyer EG, Powell JW, Haut RC. A Biomechanical investigation of ankle injury under excessive external foot rotation in the human cadaver. J Biomech Eng. 2010;132(9):091001.
30. Shrout PE, Fleiss JL. Intraclass correlations: uses in assessing rater reliability. Psychol Bull. 1979;86(2):420–8.
31. LAUGE-HANSEN N. Ligamentous ankle fractures; diagnosis and treatment. Acta Chir Scand. 1949;97(6):544–50.

32. Lee TH, Jang KS, Choi GW, Jeong CD, Hong SJ, Yoon MA, et al. The contribution of anterior deltoid ligament to ankle stability in isolated lateral malleolar fractures. Injury. 2016;47(7):1581–5.
33. Oae K, Takao M, Uchio Y, Ochi M. Evaluation of anterior talofibular ligament injury with stress radiography, ultrasonography and MR imaging. Skeletal Radiol. 2010;39(1):41–7.
34. Atilla OD, Yesilaras M, Kilic TY, Tur FC, Reisoglu A, Sever M, et al. The accuracy of bedside ultrasonography as a diagnostic tool for fractures in the ankle and foot. Acad Emerg Med. 2014;21(9):1058–61.
35. Hedelin H, Goksör L, Karlsson J, Stjernström S. Ultrasound-assisted triage of ankle trauma can decrease the need for radiographic imaging. Am J Emerg Med. 2013;31(12):1686–9.
36. Saengsin J, Vaseenon T, Pattamapaspong N, Kritsaneephaiboon A. Effectiveness of sonography assisted minimal invasive plate osteosynthesis (MIPO) compare with fluoroscope assisted in femoral shaft fracture: A cadaveric study. Injury. 2017;48(8):1758–63.
37. Hagemeijer NC, Saengsin J, Chang SH, Waryasz GR, Kerkhoffs G, Guss D et al. Diagnosing syndesmotic instability with dynamic ultrasound - establishing the natural variations in normal motion. Injury. 2020.
38. Koval KJ, Egol KA, Cheung Y, Goodwin DW, Spratt KF. Does a positive ankle stress test indicate the need for operative treatment after lateral malleolus fracture? A preliminary report. J Orthop Trauma. 2007;21(7):449–55.
39. Sanders DW, Tieszer C, Corbett B. Operative versus nonoperative treatment of unstable lateral malleolar fractures: a randomized multicenter trial. J Orthop Trauma. 2012;26(3):129–34.
40. Egol KA, Amirtharajah M, Tejwani NC, Capla EL, Koval KJ. Ankle stress test for predicting the need for surgical fixation of isolated fibular fractures. J Bone Joint Surg Am. 2004;86–a(11):2393–8.
41. Willett K, Keene DJ, Mistry D, Nam J, Tutton E, Handley R, et al. Close contact casting vs surgery for initial treatment of unstable ankle fractures in older adults: A randomized clinical trial. JAMA. 2016;316(14):1455–63.
42. Seidel A, Krause F, Weber M. Weightbearing vs gravity stress radiographs for stability evaluation of Supination-External rotation fractures of the ankle. Foot Ankle Int. 2017;38(7):736–44.
43. Holmes JR, Acker WB 2nd, Murphy JM, McKinney A, Kadakia AR, Irwin TA. A novel algorithm for isolated Weber B ankle fractures: A retrospective review of 51 nonsurgically treated patients. J Am Acad Orthop Surg. 2016;24(9):645–52.
44. Kwon JY, Cronin P, Velasco B, Chiodo C. Evaluation and significance of mortise instability in supination external rotation fibula fractures: A review Article. Foot Ankle Int. 2018;39(7):865–73.

Publisher's note